

# Characterization of Covalent Functionalized Carbon Nanotubes

Manuel G. Rüther,<sup>†</sup> Fiona Frehill,<sup>‡</sup> John E. O'Brien,<sup>§</sup> Andrew I. Minett,<sup>†</sup> Werner J. Blau,<sup>†</sup> Johannes G. Vos,<sup>‡</sup> and Marc in het Panhuis<sup>\*,#</sup>

Departments of Physics and Chemistry, Trinity College Dublin, Dublin 2, Ireland, National Centre for Sensor Research, School of Chemical Sciences, Dublin City University, Dublin 9, Ireland, and Department of Physics & NanoTech Institute, the University of Texas at Dallas, 2601 North Floyd Road, Richardson, Texas 75083

Received: March 31, 2004

The characterization of chemically modified carbon nanotubes has been achieved using  $^{13}\text{C}$  nuclear magnetic resonance (NMR) spectroscopy. Amino-functionalized multiwall carbon nanotubes (MWNT-NH<sub>2</sub>) were reacted with a  $^{13}\text{C}$  terephthalic acid. Covalent attachment of the acid to the nanotubes is confirmed by  $^{13}\text{C}$  NMR and 2D NMR through the presence of amide grouping resonances.

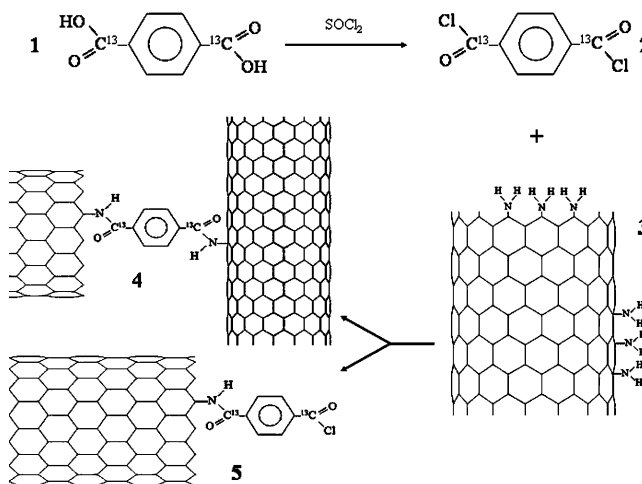
## 1. Introduction

Covalent attachment of functional groups to carbon nanotubes has received an increasing amount of attention in the past years. It is thought that covalent coupling of nanotubes to one another or to molecular entities can lead to advances in nanodevice applications such as nanosized electronics and sensing. Coupling has almost exclusively been achieved using ester or amide linkages. Amides have been the primary linkage method for nanotube interconnects,<sup>1,2</sup> the covalent attachment of proteins,<sup>3–5</sup> DNA,<sup>6,7</sup> nanocrystals,<sup>8,9</sup> and metal containing complexes.<sup>1,10–12</sup>

However, the characterization methods employed to confirm the covalent attachment between carbon nanotubes and other entities have so far provided only indirect evidence. For example, in our work on interconnecting multiwall carbon nanotubes (MWNT) using a ruthenium bridging complex,<sup>1</sup> atomic force microscopy (AFM) imaging and height analysis and UV–vis and emission spectroscopy were applied to investigate the reaction.

Characterization of carbon nanotubes before and after functionalization with small groups such as carboxylic acid (–COOH) and amino groups (–NH<sub>2</sub>) has been carried out using Raman analysis of the nanotube tangential mode,<sup>2</sup> X-ray photoelectron spectroscopy (XPS),<sup>6,13</sup> infrared spectroscopy (IR),<sup>8–10,13,14</sup> scanning tunneling microscopy (STM),<sup>1,13</sup> and nuclear magnetic resonance (NMR).<sup>14,15</sup> Results obtained from these characterization methods become increasingly difficult to interpret when larger molecular entities are attached to the functionalized groups. AFM imaging and height analysis have been employed to verify the presence of interconnected<sup>1,2</sup> and DNA-functionalized<sup>7</sup> carbon nanotubes; however, in itself, AFM only provides a visual suggestion. Attempts have also been made to use nuclear magnetic resonance (NMR) spectroscopy to characterize covalent bonding to carbon nanotubes. Wong et al. carried out  $^1\text{H}$  and  $^7\text{Li}$  NMR on  $\text{COO}^- \text{NH}_3^+$  ionically bound organic crown ethers with nanotubes<sup>16</sup> and  $^{31}\text{P}$  NMR on Vaska's compound with nanotubes.<sup>10</sup> Sun et al. employed  $^1\text{H}$  NMR spectroscopy to study esterification linkages with nanotubes<sup>17</sup> and diimide-

SCHEME 1: Reaction Scheme<sup>a</sup>



<sup>a</sup> Please note that **4** and **5** represent all forms of covalent functionalization at the nanotube sidewalls and ends.

activated amidation of nanotubes.<sup>18</sup> Hamers et al. used  $^1\text{H}$  NMR to analyze the amide linkage between dodecylamine and nanotubes.<sup>6</sup> These authors report that they have “strong evidence” for ester/amide linkages upon functionalization of carbon nanotubes. In addition, Goze-Bac et al. used  $^{13}\text{C}$  NMR to investigate covalent functionalization of  $^{13}\text{C}$ -enriched carbon nanotubes.<sup>15,19</sup>

In this work,  $^1\text{H}$ ,  $^{13}\text{C}$ , and 2D NMR is used for providing evidence of the successful chemical modification of carbon nanotubes using  $^{13}\text{C}$ -labeled terephthalic-carboxy- $^{13}\text{C}_2$  acid as the modifier (**1**, Scheme 1). It should be noted that the NMR data in ref 19 originates from carbon atoms in the nanotubes, whereas in the present work emphasis is on carbon in the attached molecules.

## 2. Experimental Details

Amino-functionalized multiwall carbon nanotubes (MWNT-NH<sub>2</sub>) were produced by catalytic chemical vapor deposition and obtained from Nanocyl S. A. (Namur, Belgium). Further details of the preparation and analysis of MWNT-NH<sub>2</sub> can be found in refs 1 and 13. Scheme 1 shows the synthesis route taken for

\* Corresponding author. E-mail: marc@utdallas.edu.

<sup>†</sup> Department of Physics, Trinity College Dublin.

<sup>‡</sup> Dublin City University.

<sup>§</sup> Department of Chemistry, Trinity College Dublin.

<sup>#</sup> The University of Texas at Dallas.

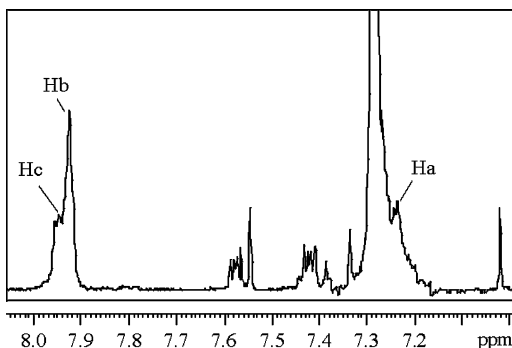


**Figure 1.**  $^1\text{H}$  NMR spectrum of the reaction product in  $\text{CDCl}_3$ .

preparing modified nanotubes. Fifty milligrams of **1** was dissolved in 15 mL of thionyl chloride. The mixture was refluxed under argon for 5 h. Thionyl chloride was subsequently removed by vacuum distillation. The compound obtained, **2**, was dissolved in  $\text{CH}_2\text{Cl}_2$ . Two milligrams of MWNT- $\text{NH}_2$ , **3**, were sonicated in 5 mL of  $\text{CH}_2\text{Cl}_2$  for 2 min. This solution was added to the **2** solution. Ten milliliters of triethylamine (TEA) was added to the solution, and the reaction mixture was stirred at room temperature for 72 h under argon. All solvents were removed by vacuum distillation, and the remaining solid was added to 5 mL of  $\text{CH}_2\text{Cl}_2$ . This solution was sonicated and then allowed to settle for 48 h. Unreacted MWNT- $\text{NH}_2$  is obtained as a solid, leaving chemically modified carbon nanotubes in solution.

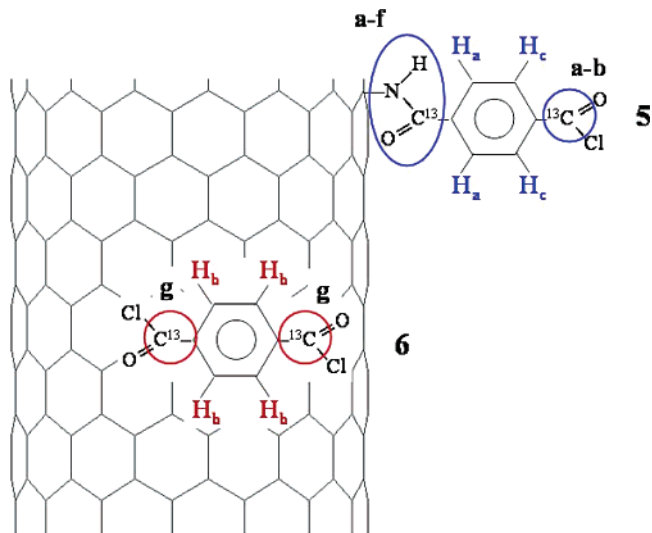
Subsequently, the top part of the solution was carefully pipetted off, the solvent taken off, and the solid obtained redissolved in  $\text{CDCl}_3$ .  $^1\text{H}$  and  $^{13}\text{C}$  NMR spectroscopy was carried out on this solution using a Bruker Avance DPX 400 MHz spectrometer. To achieve good signal-to-noise ratios the carboxy groups of terephthalic acid were labeled with 100%  $^{13}\text{C}$ . As a result nonlabeled positions show only weak signals due to the low natural  $^{13}\text{C}$  abundance of 1.1%. All  $^{13}\text{C}$  NMR spectra were recorded proton decoupled.

### 3. Results and Discussion

All NMR spectra were recorded without intensive purification of the reaction mixture. Thus, signals in the NMR spectra that correspond to the starting materials, products, and solvents can be expected. The  $^1\text{H}$  NMR spectrum of **1** in  $\text{D}_2\text{O}$ /potassium carbonate shows a singlet peak at  $\delta = 7.84$  ppm indicative of the four identical hydrogens on the phenyl ring (not shown). **1** is insoluble in  $\text{CDCl}_3$ , and therefore it is not expected to feature in the NMR spectrum of the reaction mixture.

The  $^1\text{H}$  NMR spectrum of **2** (in  $\text{CDCl}_3$ ) shows one peak at  $\delta = 8.04$  ppm with a half line width of 2.6 Hz corresponding to the presence of four equivalent aromatic protons (not shown). The  $^1\text{H}$  NMR spectrum of the reaction mixture (Figure 1 and Figure S1 in the Supporting Information) shows one broad peak at  $\delta = 7.92$  ppm ( $\text{H}_b$ ) and two multiplets at  $\delta = 7.95$  ppm ( $\text{H}_c$ ) and  $\delta = 7.23$  ppm ( $\text{H}_a$ ). The other peaks (in Figure 1) can be attributed to solvent ( $\delta = 7.28$  ppm) and vacuum grease contamination which occurred during the drying process in the NMR sample preparation. The appearance of line broadening suggests that a reaction with the amino groups attached on the nanotube surface occurred. The appearance of two signals at  $\delta = 7.95$  and  $\delta = 7.23$  ppm is indicative of the presence of an asymmetric substituted 1,4-phenylene derivative<sup>20</sup> and is consistent with the presence of **5**. Scheme 2 shows the proposed assignment for the phenylene protons of product **5**. One end of the phenylene ring is connected via an amide group to the

**SCHEME 2: Proposed Proton ( $\text{H}_a$ – $\text{H}_c$ , Figure 1) and Carbonyl Carbon (a–g, Figure 2) Assignment in the Reaction Product<sup>a</sup>**



<sup>a</sup> **5** indicates covalent functionalization, whereas **6** indicates non-covalent sidewall functionalization (coating) of MWNT with **2**.

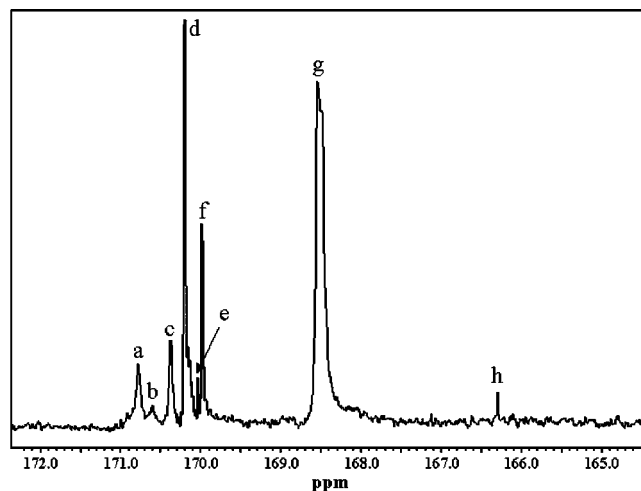


**Figure 2.**  $^{13}\text{C}$  NMR spectrum of the reaction product in  $\text{CDCl}_3$ . Peak positions are indicated by a–h.

MWNT whereas the other end carries an acyl chloride group (Schemes 1 and 2). The signal at  $\delta = 7.92$  ppm ( $\text{H}_b$ ) is indicative of a symmetric arrangement of protons and agrees well with the value obtained for **2** given above.

In the  $^{13}\text{C}$  NMR spectrum of the reaction mixture (Figure S2 in the Supporting Information), four large peak areas can be identified around 8, 45, 77, and 170 ppm. These areas are indicative of TEA methyl ( $-\text{CH}_3$ ), TEA alkylamine ( $-\text{NHCH}_2-$ ), solvent ( $\text{CDCl}_3$ ), and carbon carbonyl ( $-\text{CO}-$ ) groups, respectively. Figure 2 shows the carbonyl region in the  $^{13}\text{C}$  NMR spectrum of the reaction product. As noted before, the starting material **1** is insoluble in  $\text{CDCl}_3$  and is therefore unlikely to feature.<sup>21</sup>

The peaks in Figure 2 correspond to the labeled carbonyl carbons only. It is not straightforward to assign these peaks to a specific nanotube assembly; however, their appearance does confirm covalent bonding. Let us now address which NMR signals could be expected from the reaction product. If both active sides of **2** would react with **3**, then **4** is obtained as the product and only acyl amide type signals are expected. However, if just one active side reacts with the amino-functionalized

nanotubes, giving **5** as product, a carbon signal indicative of acyl chloride should also be detected.

For **2** in  $\text{CDCl}_3$  a  $^{13}\text{C}$  NMR signal at  $\delta = 167.50$  ppm was recorded. Therefore, it is reasonable to assume that signal **g** ( $\delta = 168.54$ ) is indicative of acyl chloride ( $\text{ClCO}$ –phenyl). A more detailed analysis of signal **g** reveals that there are at least three signals together forming one broad signal. The  $\text{sp}^2$  nature of the nanotubes has a deshielding effect on the carbonyl carbons, which leads to a downfield shift of the corresponding signal in the  $^{13}\text{C}$  NMR. It has been shown that  $\pi$ -conjugated molecules can render nanotubes soluble through noncovalent sidewall functionalization ( $\pi$ -stacking).<sup>22</sup> In Scheme 2, **6** indicates  $\pi$ -stacking of **2** onto MWNT. The (nanotube)  $\text{sp}^2$  deshielding effect would result in a downfield shift for **6** ( $\pi$ -stacked component **2**), compared with  $\delta = 167.50$  ppm **2** in  $\text{CDCl}_3$ . Therefore, it is assumed that signal **g** could originate from the acyl chloride in **6**.

The carbonyl  $^{13}\text{C}$  resonance in dimethyl-substituted amide ( $\text{CH}_3\text{--NHCO--CH}_3$ ) in  $\text{CDCl}_3$  has a chemical shift of  $\delta = 171.60$  ppm<sup>23</sup> for the carbonyl carbon. Through comparison with other established shifts for amides,<sup>23</sup> it can be deduced that substitution of  $\text{sp}^2$  systems results in the following shift changes. Substitution on the nitrogen side (phenyl–NHCO– $\text{CH}_3$ ) results in a shielding effect which would result in an upfield shift of the signal, whereas substitution on the carbon side ( $\text{CH}_3\text{--NHCO--phenyl}$ ) results in a deshielding effect which would result in a downfield shift of the signal. It should be noted that the signal shift caused by deshielding is smaller compared to the signal shift caused by shielding. Thus, an upfield shift (lower ppm) can be expected for MWNT–NHCO–phenyl in comparison with the 171.60 ppm shift recorded for  $\text{CH}_3\text{--NHCO--CH}_3$ . We can therefore conclude that the peaks **a–f** are indicative of the presence of amide bonds and modified MWNT. The small differences in shifts between peaks **a–f** could be indicative of the presence of different local environments in **4** and/or **5**.

2D NMR correlation spectroscopy can provide further useful information about the nature of the signals obtained. The heteronuclear multiple bond connectivity (HMBC) experiment allows the investigation of atoms of long-range coupling between protons and carbons. Figure 3 shows the HMBC spectrum of the reaction mixture in  $\text{CDCl}_3$ .

The correlation regions in the HBMC spectrum can be explained as follows. To identify the correlation regions (CR) the following notation is adopted: (proton peak; carbon peak). The coordinates for the correlation region centers are: CR1 (7.92; 168.5), CR2 (7.23; 170.2), and CR3 (7.95; 171.0). In CR1, the symmetric aromatic proton ( $\text{H}_b$ ) is correlated with carbon in the range of 167.5–169.9 ppm and centered on peak **g**. This is consistent with signals arising from the presence of **6**, as shown in Scheme 2. In CR2, the asymmetric aromatic proton ( $\text{H}_a$ ) is correlated with carbon in the range of 169.5–171.0, corresponding to peaks **a–f**. This is consistent with signals arising from the carbon participating in the amide bond of **5** as shown in Scheme 2. In CR3, the asymmetric aromatic proton ( $\text{H}_c$ ) is correlated with carbon in the range of 170.5–171.5 ppm, corresponding to peaks **a** and **b**. This is consistent with signals arising from the carbon in the acyl chloride part of **5** as shown in Scheme 2. The presence of the two correlation regions (CR2 and CR3) is a direct indication that assembly **5** was formed during the reaction. Asymmetric protons are correlated with carbons in different carbonyl environments.

Signals originating from **4** could not be assigned, due most likely to the low concentration of this compound.

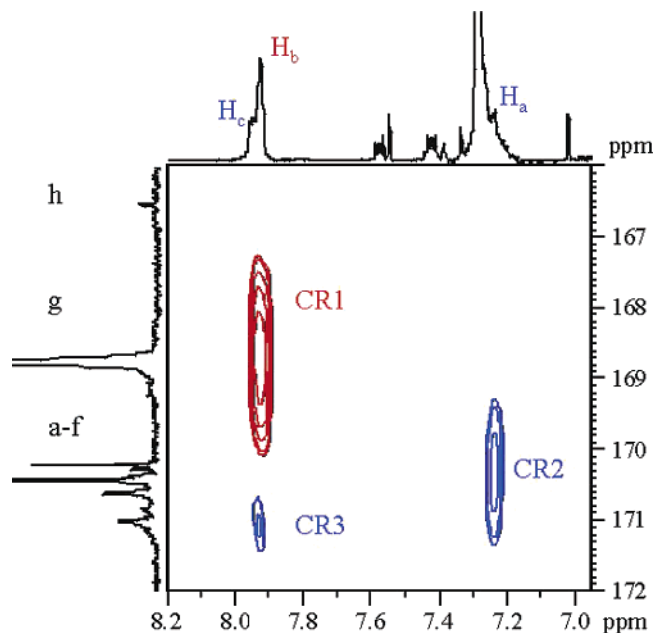


**Figure 3.** HMBC spectrum of the reaction product in  $\text{CDCl}_3$ . CR1–CR3 indicate correlation regions, whereas  $\text{H}_a$ – $\text{H}_c$  indicate peaks in the  $^1\text{H}$  NMR spectrum (see Figure 1) and **a–h** indicate peaks in the  $^{13}\text{C}$  NMR spectrum (see Figure 2).

#### 4. Conclusions

In conclusion, we have presented evidence of the chemical (covalent) bond formed between carbon nanotubes and a  $^{13}\text{C}$ -labeled molecule. With the use of  $^1\text{H}$  NMR,  $^{13}\text{C}$  NMR, and the 2D (HMBC) correlation spectrum, signals for the (amide) linkage between terephthalic acid (labeled molecule) and MWNT could be assigned.

It was possible to identify (asymmetric) NMR signals originating from labeled molecules bound to MWNT. NMR correlation regions could be attributed to amide linkage and acyl chloride parts of product **5**. In addition, signals originating from **6** (noncovalent functionalization of MWNT with **2**) could be assigned.

We envisage that combination of NMR experiments can become a useful tool in the characterization of chemical bonds between carbon nanotubes and molecular entities, leading to advances in molecular sensing and electronics.

**Acknowledgment.** F.F. and J.G.V. thank Enterprise Ireland for financial assistance.

**Supporting Information Available:**  $^1\text{H}$  and  $^{13}\text{C}$  spectra of the reaction product in  $\text{CDCl}_3$ . This material is available free of charge via the Internet at <http://pubs.acs.org>.

#### References and Notes

- (1) Frehill, F.; Vos, J. G.; Benrezzak, S.; Koós, A. A.; Kónya, Z.; Rüther, M. G.; Blau, W. J.; Fonseca, A.; Nagy, J. B.; Biró, L. P.; Minett, A. I.; in *het Panhuis, M. J. Am. Chem. Soc.* **2002**, *124*, 13694.
- (2) Chiu, P. W.; Duesburg, G. S.; Dettlaff-Wegiikowska, U.; Roth, S. *Appl. Phys. Lett.* **2002**, *80*, 3811.
- (3) Huang, W.; Taylor, S.; Fu, K.; Lin, Y.; Zhang, D.; Hanks, T. W.; Rao, A. M.; Sun, Y.-P. *Nano Lett.* **2002**, *2*, 311.
- (4) Fu, K.; Huang, W.; Lin, Y.; Zhang, D.; Hanks, T. W.; Rao, A. M.; Sun, Y.-P. *J. Nanosci. Nanotechnol.* **2002**, *2*, 457.
- (5) Lin, Y.; Taylor, S.; Li, H.; Fernando, K. A. S.; Qu, L.; Wang, W.; Gu, L.; Zhou, B.; Sun, Y.-P. *J. Mater. Chem.* **2004**, *14*, 527.
- (6) Baker, S. E.; Cia, W.; Lasseter, T. L.; Weidkamp, K. P.; Hamers, R. J. *Nano Lett.* **2002**, *2*, 1413.
- (7) Williams, K. A.; Veenhuizen, P. T. M.; de la Torre, B. G.; Eritja, R.; Dekker, C. *Nature* **2002**, *420*, 761.
- (8) Banerjee, S.; Wong, S. S. *Nano Lett.* **2002**, *2*, 195.

- (9) Haremza, J. M.; Hahn, M. A.; Krauss, T. D.; Chen, S.; Calcines, J. *Nano Lett.* **2002**, 2, 1253.
- (10) Banerjee, S.; Wong, S. S. *Nano Lett.* **2002**, 2, 49.
- (11) Banerjee, S.; Wong, S. S. *J. Am. Chem. Soc.* **2002**, 124, 8940.
- (12) Ravindran, S.; Chaudhary, S.; Colburn, B.; Ozkan, M.; Ozkan, C. S. *Nano Lett.* **2003**, 3, 447.
- (13) Kónya, Z.; Vesselenyi, I.; Niesz, K.; Kukovecz, A.; Demortier, A.; Fonseca, A.; Delhalle, J.; Mekhalif, Z.; Nagy, J. B.; Koós, A. A.; Osváth, Z.; Kocsonya, A.; Biró, L. P.; Kirisci, I. *Chem. Phys. Lett.* **2002**, 360, 429.
- (14) Chen, J.; Hamon, M. A.; Hu, H.; Chen, Y.; Rao, A. M.; Eklund, P. C.; Haddon, R. C. *Science* **1998**, 282, 95.
- (15) Goze-Bac, C.; Bernier, P.; Latil, S.; Jourdain, V.; Rubio, A.; Jhang, S. H.; Lee, S. W.; Park, Y. W.; Holzinger, M.; Hirsch, A. *Curr. Appl. Phys.* **2001**, 1, 149.
- (16) Kahn, M. G. C.; Banerjee, S.; Wong, S. S. *Nano Lett.* **2002**, 2, 1215.
- (17) Fu, K.; Huang, W.; Lin, Y.; Riddle, L. A.; Carroll, D. L.; Sun, Y.-P. *Nano Lett.* **2001**, 1, 439.
- (18) Fu, K.; Kitaygorodskiy, A.; Rao, A. M.; Sun, Y.-P. *Nano Lett.* **2002**, 2, 1165.
- (19) Goze-Bac, C.; Latil, S.; Lauginie, P.; Jourdain, V.; Conard, J.; Duclaux, L.; Rubio, A.; Bernier, P. *Carbon* **2002**, 40, 1825.
- (20) Williams, D. H.; Fleming, I. *Spectroscopic Methods in Organic Chemistry*, 5th ed.; McGraw-Hill: New York; London, 1995.
- (21) When the starting product **1** was dissolved in a solvent mixture of D<sub>2</sub>O/potassium carbonate, a <sup>13</sup>C NMR shift of 174.84 ppm was recorded for the carboxylic acid carbon.
- (22) in het Panhuis, M.; Maiti, A.; Dalton, A. B.; van den Noort, A.; Coleman, J. N.; McCarthy, B.; Blau, W. J. *J. Phys. Chem. B* **2003**, 127, 478.
- (23) Levy, G. C.; Lichter, R. L.; Nelson, G. L. *Carbon-13 Nuclear Magnetic Resonance Spectroscopy*, 2nd ed.; John & Sons: New York, 1980.